Journal of Natural Gas Science and Engineering 96 (2021) 104298

Contents lists available at ScienceDirect

Journal of Natural Gas Science and Engineering

journal homepage: www.elsevier.com/locate/jngse

A sequential decision and data analytics framework for maximizing value and reliability of CO_2 storage monitoring

Amine Tadjer *, Aojie Hong, Reidar B. Bratvold

Univerisity of Stavanger, Norway

ARTICLE INFO

Keywords:
Value of information
CO_2 storage monitoring
Approximate dynamic programming
Machine learning
Time-lapse seismic monitoring

ABSTRACT

Carbon capture and sequestration (carbon capture and storage or CCS) represents a unique potential strategy that can minimize CO_2 emissions in the atmosphere, and it creates a pathway toward a neutral carbon balance, which cannot be solely achieved by combining energy efficiency and other forms of low carbon energy. To contribute to the decision-making process and ensure that CCS is successful and safe, an adequate monitoring program must be implemented to prevent storage reservoir leakage and contamination of drinking water in groundwater aquifers. In this paper, we propose an approach to perform value of information (VOI) analyses to address sequential decision problems in reservoir management in the context of monitoring the geological storage of CO_2 operations. These sequential decision problems are often solved and modeled by approximate dynamic programming (ADP), which is a powerful technique for handling complex large-scale problems and finding a near-optimal solution for intractable sequential decision-making. In this study, we tested machine learning techniques that fall within ADP to estimate the VOI and determine the optimal time to stop CO_2 injections into the reservoir based on information from seismic surveys. This ADP approach accounts for both the effect of the information obtained before a decision and the effect of the information that might be obtained to support future decisions while significantly improving the timing, value of the decision, and uncertainty of the CO_2 plume behavior, thereby significantly increasing economic performance. The Utsira saline aquifer west of Norway was used to exemplify ADP's ability to improve decision support regarding CO_2 storage projects.

1. Introduction

Carbon capture and storage (CCS) is increasingly considered a promising strategy for reducing CO_2 emissions. Geological reservoirs, such as depleted oil or gas fields or deep saline aquifers, are being considered as appropriate geological formations that can store CO_2 emissions at a depth of several thousand meters (Harp et al., 2017; Jin et al., 2017; Nilsen et al., 2015a). However, uncertainties in geological models and rock properties affect flow modeling and CO_2 storage capacities, mitigating the risk of CO_2 leakage and contaminating clean groundwater. To contribute to the decision-making process and ensure that CCS is successful and safe, a monitoring program must be implemented in addition to regulations based on conformance (understanding of CO_2 behavior), containment (ensuring control of CO_2 migration), and contingency (detecting and addressing significant anomalies and leakages) (Dupuy et al., 2017). Several studies have demonstrated the utility of applying time-lapse seismic and electromagnetic surveys to adequately monitor CO_2 storage in geological formations. For instance, seismic surveys of the Sleipner storage site have been conducted regularly. From these surveys, a large quantum of data has become accessible for research, resulting in several published studies (for instance, (Arts et al., 2004; Dupuy et al., 2017; Furre et al., 2017)). Furre et al. (2017) summarized 20 years of monitoring CO_2 injection at Sleipner. The authors concluded that the monitoring program at Sleipner, which is strongly reliant on seismic surveys, has been successful, with CO_2 contained safely in the storage unit. However, since time-lapse seismic data are costly, it is important to assess their impact on the necessary decisions and design monitoring programs effectively to optimize the relationship between value and cost. One possible method of estimating the value of a monitoring scheme is the decision-analytic metric of the value of information (VOI) (Howard, 1966). VOI is an estimate of the additional value that information brings to a decision situation (Howard, 1966). If the prospect values linked to the different decision alternatives are specified in monetary units, the VOI provides a monetary calculation of the additional value of data collection before deciding. From a decision-analytical viewpoint, information is useful not only if it eliminates uncertainty but also if it promotes better decisions and maximizes value results by reducing uncertainty. In the context of underground reservoir management, the

* Corresponding author.
E-mail address: amine.tadjer@uis.no (A. Tadjer).

https://doi.org/10.1016/j.jngse.2021.104298
Received 29 April 2021; Received in revised form 27 September 2021; Accepted 20 October 2021
Available online 6 November 2021

concept of VOI has been applied to decision analysis in petroleum exploration and production (Newendorp, 1975; Riis, 1999). The importance of seismic information has been studied regularly. Decision tree models have been used to measure the economic effect of seismic imaging on reservoir management (Bickel et al., 2008). Although seismic information is considered imperfect, a significant value can be extracted from this information. Furthermore, Bickel et al. (2008) introduced a general VOI model that can drive multiple objectives, budgetary limitations, and quantitative models relating seismic parameters to reservoir properties. The decision model also provides objective estimates of seismic measurement reliability. In addition, (Bratvold et al., 2009) extensively reviewed the application of VOI in petroleum exploration and formed a rather interesting argument. In Eidsvik et al. (2015) work, VOI analysis was integrated with geostatistical modeling to provide applications for the petroleum industry as well as mining and groundwater management.

In general, applications of VOI analyses in the context of CCS operation monitoring are limited. For instance, Sato (2011) provided two demonstrations of VOI applied to the CO_2 sequestration problem. The first example considered a storage reservoir with a fault (potential leak-pathway), followed by a cross-well interference test conducted to determine whether the fault is tight or permeable. A discrete probability was assigned to the reliability of the test. The second example considered a continuous uncertainty: the net present value (NPV) of the project was linked to the radial extent of the saline aquifer, which was assumed to be lognormally distributed. The accuracy of the information gathering was not based on empirical data, but rather assumed to be described by a triangular probability density function. Puerta-Ortega et al. (2013) later extended Sato's work; they quantified VOI by prior scenarios based on the reservoir's current knowledge, contractual conditions, and regulatory constraints.

In real-world applications, the analytical calculation of the VOI is generally challenging. Therefore, a computationally efficient approach to estimate the VOI in such cases is the approximate dynamic programming (ADP), which is presented and used in the field of financial engineering with real options (Longstaff and Schwartz, 2001; Jafarizadeh and Bratvold, 2009). Hong et al. (2018a) illustrated a specific method for ADP, the least-squares Monte Carlo (LSM) algorithm. This approach uses Monte Carlo sampling and statistical regression techniques to estimate the VOI. This algorithm can be implemented with a production model based on exponential declines to determine the optimal time to switch from one recovery phase to another. Theoretically, the implementation of LSM is independent of production models; however, LSM still suffers from dimensionality in the action space, where the computational effort of LSM increases exponentially with the number of both alternatives and decision points. Eidsvik et al. (2017), Dutta et al. (2019) used a simulation-regression approach to approximate the VOI; an ensemble was used as part of this approach to compute the predicted values directly. Anyosa et al. (2021) developed a statistical learning method to assess the probability of an early CO_2 leakage detection through a key fault at the Smeaheia site and then conducted a VOI analysis of monitoring strategies, considering an underlying decision situation connected to continued injection of CO_2, or termination of this process. In this setting, geophysical monitoring is valuable if it leads to improved decisions for the injection program.

Our approach in the current study is different from that of Anyosa et al. (2021). Specifically, a decision problem is constructed where CO_2 is injected into a reservoir and the decision-maker conducts seismic surveys to decide between continuing or stopping the injection based on information from the survey results. The actual VOI calculation in our case was computed using the ADP methodology. The ADP methodology used here illustrates both the impact of the seismic survey data obtained before a decision is made and the effect of the data information that can be obtained to support future decisions. The analysis was performed on a constructed case study involving the Utsira storage site. Further, we use a machine learning regression approach that lies within the domain of ADP to estimate the VOI and determine the optimal time to stop the CO_2 injections into the reservoir.

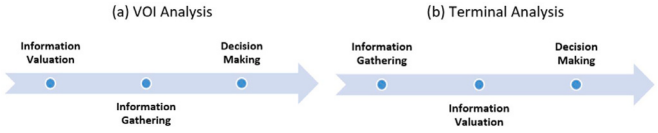

Fig. 1. Steps of a – VOI analysis, and b – Terminal analysis.

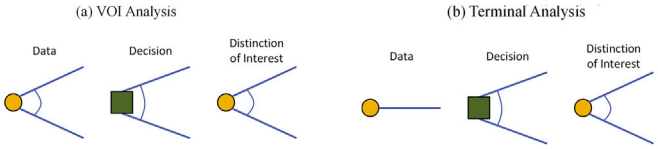

Fig. 2. Decision tree elements of VOI versus terminal analysis Hong et al. (2018b).

This paper is divided into multiple sections. In the following section, we distinguish between the VOI and terminal analysis, define VOI, and present the general steps in terms of its assessment. Next, we present the Utsira Formation along with the methods used to generate seismic data. Subsequently, we present a complete methodology for assessing the VOI using machine learning methods and then test the proposed methodology by implementing it in the Utsira reservoir fields. Finally, we offer concluding remarks and recommendations for future research directions.

2. Background

In this section, we provide a brief background of the VOI analysis. We also introduce the Utsira saline aquifer along with the standard approach employed to estimate model 4D seismic data.

2.1. Decision analysis and VOI in the energy industry

Decision analysis has been extensively used in the energy industry since the 1960s. Bratvold et al. (2009) identified several papers in the O&G literature that present cases where the information value is calculated after the information has been gathered. This can take the form of historical lookbacks to document the impact of information (Aylor Jr., 1999; Waggoner, 2000). Raiffa and Schlaifer (1961) referred to this as "terminal analysis". Terminal analysis involves the evaluation of selection between alternatives after a test (actual or hypothetical) has been conducted and the data have been gathered, whereas VOI analysis, often called "preposterior analysis" (Raiffa and Schlaifer, 1961), regards the decision problem as it appears before a test has been conducted. Fig. 1 illustrates the stages of VOI and terminal analyses. Fig. 2 depicts the decision-tree elements of VOI versus terminal analysis, where the circles and squares represent the uncertainty and decision nodes, respectively. The data of concern in a VOI analysis (Fig. 2a) are future data, which are unknown and treated as uncertain. In contrast, the data of concern in terminal analysis (Fig. 2b) are historical data, which are already known and treated as certain.

Although a terminal analysis might offer valuable insights, it is not a replacement for VOI analysis. Furthermore, it introduces bias for two reasons. First, from a communication and publishing perspective, there is a strong incentive to not publish or communicate unsuccessful (those unable to demonstrate any value creation) information-gathering activities. Second, it ignores cases in which information was not gathered but should have been.

VOI in any information-gathering activity depends on two fundamental uncertainties: (1) the uncertainties we hope to learn about but cannot directly observe; these are called "events of interest", and (2)

the test results referred to as observable distinctions (Bratvold et al., 2009). In reservoir management, the data gathered until time t when a decision is made is the observable distinction, and prediction after the time t runs out constitutes the event of interest. We denote the observable distinction as x. Since x has very high dimensions, it is difficult to represent the distribution of x in an analytical form because we usually approximate it with the help of Monte Carlo sampling. In terms of a risk-neutral decision maker, VOI is defined as follows:

$$VOI = \begin{bmatrix} Expected\ value\ with \\ additional\ information \end{bmatrix} - \begin{bmatrix} Expected\ value\ without \\ additional\ information \end{bmatrix}$$

In mathematical form,

$$VOI = \{0, \Delta\} \tag{1}$$

$$\Delta = EVWII - EVWOI \tag{2}$$

The lower limit of VOI is always 0 because if Δ is negative when $EVWOI > EVWII$, the decision-maker can always choose not to gather information.

In a decision-making context, the decision without information (DWOI) is the alternative that optimizes the expected value (EV) over the prior, and $EVWOI$ is the optimal EV over the prior.

$$EVWOI = max_{a\in A}\left[\int v(x,a)p(x)dx\right] \approx max_{a\in A}\left[\frac{1}{b}\sum_{b=1}^{B} v(x^b,a)\right] \tag{3}$$

where a is the decision alternative from the a set of A, x is the distinctions of interests, $v(x,b)$ is the value function that assigns a value to each alternative outcome pair for a given x and realization b, and $p(x)$ is the prior probability distribution of x.

Similarly, if we have perfect information regarding what value x the distinction of interests will assume, we can choose the optimal action for that value of x. The decision with information (DWI) is an alternative that optimizes the expected value over the posterior.

$$EVWII = \int max_{a\in A}[E(v(x,a)|y)]p(y)dy \approx \frac{1}{B}\sum_{b=1}^{B} max_{a\in A}E[v(x,a)|y^b] \tag{4}$$

Where $p(y)$ is the marginal probability distribution over y.

Furthermore, the decision with perfect information (DWPI) can also be determined in this decision-making context. For instance, in reservoir engineering, perfect information is the information that reveals the true reservoir properties and impacts of the recovery mechanism. Considering the CO_2 injection operation problem as an example, the EV with perfect information (EVWPI) is the maximum NPV for every path based on prior realizations or distributions. Averaging these NPVs over the paths would result in $EVWPI$. In this respect, every path has its optimal decision with perfect information. The difference between $EVWPI$ and $EVWOI$ is the value of perfect information (VOPI).

2.2. Utsira CO_2 storage

Utsira is a saline reservoir located beneath the central and northern North Sea as shown in Fig. 3. In this location, there are over 20 reservoir formations (producing or abandoned oil and gas fields and geological formations such as saline aquifers). We used the reservoir dataset provided by the Norwegian Petroleum Directorate, which consists of only top-surface and thickness maps and average rock properties. The Utsira Formation consists of weakly consolidated sandstone with interlayered shale beds that act as baffle for the upward migration of the injected CO_2, and it has an average top-surface depth of approximately 800 m below the seabed (within the range of 300–1400 m). The storage capacity of the Utsira system is estimated to be 16 Gt, with a prospectivity of 0.5–1.5 Gt (Andersen et al., 2014). The boundaries of the aquifers were considered open. An open boundary means that

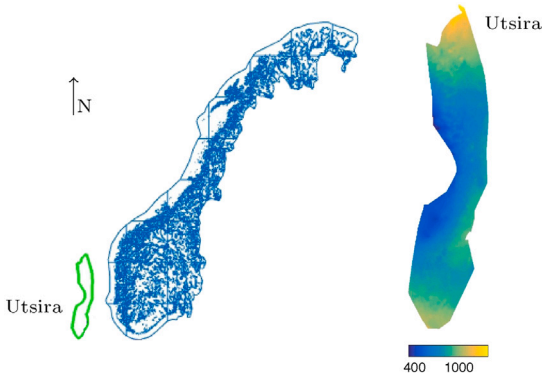

Fig. 3. Location of Utsira formation along the Norwegian Continental Shelf (left). Maps of geomodel depths in meters (below the seabed) (right) (Allen et al., 2018).

there is communication between the aquifer and anything that lies adjacent to it, be it another aquifer or the sea bottom. The corresponding permeabilities in the Utsira geomodel range from 0.5–2.5 darcys. Another study (Singh et al., 2010) suggested that permeability could be within the range of 1.1–5 darcys. Furthermore, the NCS public datasets contain no information about possible leakage through open boundaries or the caprock. We acknowledge that these are important factors, but despite these limitations, we decided to use the Utsira available data to demonstrate the ADP framework and discuss its advantages and potential benefits in future CCS operations. In our study, some of the injected CO_2 can leave the computational domain during the simulation; these are considered as leaked volumes. Nonetheless, this cannot result in CO_2 leaking into the atmosphere; in most instances, it will continue to migrate beyond the simulation model inside the rock volume.

2.3. Rock physics model and 4D seismic data

The most favorable reservoir conditions for seismic monitoring can be calculated by forward modeling of the seismic response to long-term CO_2 storage. This study includes a mathematical model that can indicate the impact of fluid and mineral substitution and the effect of porosity changes on the seismic properties of the reservoir, resulting in subsequent variations in the seismic wave velocities of the rock. To describe the changes in seismic velocity, we used the Gassmann model (Gassmann, 1951), which is more effective than other models, such as Krif's, Duff Mindlin's, and Wyllies' time-average models because of its simplicity and clarity (Nguyen and Nam, 2011). The Gassmann model can be used to calculate seismic velocities using the bulk module, which is ultra sensitive to fluid saturation variation (Han and Batzle, 2004).

The p-wave velocity of a saturated rock can be measured on the bulk modulus, shear modulus μ_{sat} and the density ρ_{sat} of the rock, and the s-wave velocity depends on ρ and μ_{sat}. The interaction was given by Avseth et al. (2005).

$$v_p = \sqrt{\frac{K_{sat} + \frac{4}{3}\mu_{sat}}{\rho_{sat}}} \tag{5}$$

$$v_s = \sqrt{\frac{\mu_{sat}}{\rho_{sat}}} \tag{6}$$

Considering the porosity value ϕ, the Gassmann equation is used to calculate the bulk modulus K_{sat} as follows:

$$K_{sat} = K_d + \frac{(1 - K_d/k_m)^2}{\frac{\phi}{k_f} + \frac{1-\phi}{k_m} + \frac{k_d}{k_m^2}} \tag{7}$$

K_d, K_m, and K_f are bulk moduli of dry rock, solid matrix, and pore fluid, respectively. The shear modulus μ_{sat} is dependent only on the

shear modulus of dry rock μ_d at generally low frequencies (since the shear modulus of a fluid is zero), considering the following:

$$\mu_{sat} = \mu_d \tag{8}$$

The density of a saturated rock can be calculated as follows:

$$\rho = \phi\rho_f + (1 - \phi_{mi}) \tag{9}$$

where ρ_f is the fluid density and ϕ_m is the mineral density.

Since porosity, density, and moduli including K_d, K_m and μ_d of the core are known or measured before the core flooding experiment, we can obtain V_p after calculating the values of K_f and ρ_f of the core.

As there are two different pore fluids (water and CO_2) in CO_2-injected reservoirs, one should further consider measuring the bulk modulus K_f and fluid density ρ_f, yet part of the injected CO_2 is dissolved in the pore water. We considered only the pore fluid as a mixture of pure water and pure CO_2 for convenience, meaning that $S_{CO_2} + S_w = 1$.

For the computation of K_f, we use Wood's equation (Wood, 1941):

$$\frac{1}{K_f} = \frac{S_w}{K_w} + \frac{(1 - S_w)}{K_{CO_2}} \tag{10}$$

where K_w and K_{CO_2} are the bulk moduli of water and CO_2, respectively. The bulk density of the fluids rho_f can be obtained as a weighted average with respect to water saturation S_w:

$$\rho_f = S_w\rho_w + (1 - S_w)\rho_{CO_2} \tag{11}$$

where ρ_w and ρ_{CO_2} are the densities of water and CO_2, respectively.

As CO_2 is injected into a reservoir, S_w decreases to change the values of K_f and ρ_f, and thus, also V_p. Therefore, we can estimate S_w and S_{CO_2} by monitoring V_p.

In the current study, we aimed to use seismic data to map the CO_2 plume within a reservoir. We assumed the elastic properties to be homogeneous in the individual layers. Each layer has elastic properties such as p-wave velocity V_p, s-wave velocity V_s, and bulk density ρ. Furthermore, we assumed that the elastic properties when the rock is saturated only by brine are known, and they are denoted as V_P^1, V_S^1, and ρ^1. The new values of the elastic properties, after CO_2 has partially replaced the brine, are denoted as V_P^2, V_S^2, and ρ^2.

For conventional Amplitude versus offset (AVO) analysis, the AVO responses are approximated by linear trigonometric functions of the offset or angle. An approximate way to describe the relationship between R and G is given by Avseth et al. (2005):

$$R(\theta) \approx R_0 + Gsin^2\theta \tag{12}$$

where R_0 (intercept) and G (curvature) are AVO attributes that depend on elastic properties at a given point in the subsurface. Let $\Delta V_p = V_{p2} - V_{p1}$ and $V_pm = (V_{p2} + V_{p1})/2$ (arithmetic mean). We define similar quantities of V_s and ρ. Approximate relationships between the AVO attributes and elastic properties were given by Avseth et al. (2005):

$$R_0 = \frac{1}{2}\left(\frac{\Delta V_p}{\Delta V_{pm}} + \frac{\Delta\rho}{\Delta\rho_m}\right) \tag{13}$$

$$G = \frac{1}{2}\frac{\Delta V_p}{\Delta V_{pm}} - 2\left(\frac{V_s}{V_p}\right)^2\left(2\frac{\Delta V_s}{\Delta V_{sm}} + \frac{\Delta\rho}{\Delta\rho_m}\right) \tag{14}$$

The AVO attributes for a given point can be estimated by recording the seismic amplitudes at different reflection angles.

3. Value computation by ADP

We used an ADP method called the simulation-regression (or LSM) method to calculate the expected value with imperfect information. The simulation regression method involves Monte Carlo simulation and regression for approximately calculating the conditional expected value of given data.

Monte Carlo simulation:

1. Numerous possible realizations of state variables (x^b) such as porosity permeability, temperature, pressure and caprock elevation are generated using Monte Carlo simulation model.
2. Forward modeling is performed to generate modeled AVO attributes data, with the addition of random noises generated from the statistics measurements errors to the modeled AVO data.
3. For each decision alternative a, the $NPV(x^b, a)$ is calculated.
4. The EVWOI is then calculated using the following equation:

$$EVWOI = \left[\frac{1}{b}\sum_{b=1}^{B} NPV(x^b, a^*_{DWOI})\right]$$

$$a^*_{DWOI} = argmax_{a\in A}\left[\frac{1}{b}\sum_{b=1}^{B} NPV(x^b, a)\right]$$

Where a^*_{DWOI} is the optimal decision without information and it is identical to each realization.

Backward induction

1. Starting recursively from the last decision point in time, to estimate the expected NPV (ENPV) with alternative a conditional on the modeled AVO data, $ENPV(x, a)|y$, we regress $[NPV_{1j}, NPV_{2j}, \ldots, NPV_B(x, a)]$ on the AVO data. This procedure is repeated for each of the alternatives.
2. The optimal scenario was then determined by selecting the option that achieves the highest NPV value, given the known information. The EVWII is then as follows:

$$EVWII = \frac{1}{b}\sum_{b=1}^{B} NPV(x^b, a^*_{DWII}(y^b))$$

$$a^*_{DWII}(y^b) = arg\frac{1}{b}\sum_{b=1}^{B} max_{a\in A} E[NPV(x^b, a)|y^b]$$

$a^*_{DWII}(y^b)$ is the optimal decision with given information y^b

3. Finally, the VOI is given by $max\{0, EVWII - EVWOI\}$.

The process of ADP is further detailed in Hong et al. (2018a,b), Longstaff and Schwartz (2001).

Since the dimensions of the time-lapse data are much larger than the number of realizations, simple regression techniques, such as linear regression, do not work in this case. Instead, we used nonlinear regression.

4. VOI for time-lapse seismic data in the utsira field CO_2 storage

4.1. Decision problem definition

With regard to the problem setting of this example, we assumed that the Utsira reservoir has one injection well at a depth of 1012 m; then, an injection rate of 10 Mt per year is considered for a period of 40 years, followed by a 3000-year migration (post-injection) period. Every flow simulation was performed using the open-source software MRST-CO_2 lab developed by Sintef (Lie, 2019). We considered two options: continuing or stopping the injection. We then analyzed the optimal time to stop the injection based on seismic surveys, which have the highest value when detecting a potential leakage of CO_2. This analysis provides useful insights into the reservoir development plan, and the decision affects learning occurring over time. A total of N=100 prior geological realizations were generated using a normal Gaussian distribution. Here, there is uncertainty in permeability, porosity, temperature, pressure, and caprock elevation. Following the case study by Nilsen et al. (2015a), which tested the sensitivity of CO_2 migration to many input parameters, it was found that porosity differences would influence the total volume of rock with which the plume comes into contact. Increasing the thickness of the pore decreases the overall volume of the rock occupied by the plume, reducing the migration so that the plume does not move far. Permeability impacts the behavior of the CO_2 plume flow by changing its speed and direction, creating a thinner plume that reaches further upslope. As shown in Fig. 4, uncertain aquifer temperature and pressure may also affect the density of CO_2, which further impacts the plume migration and storage ability estimates.

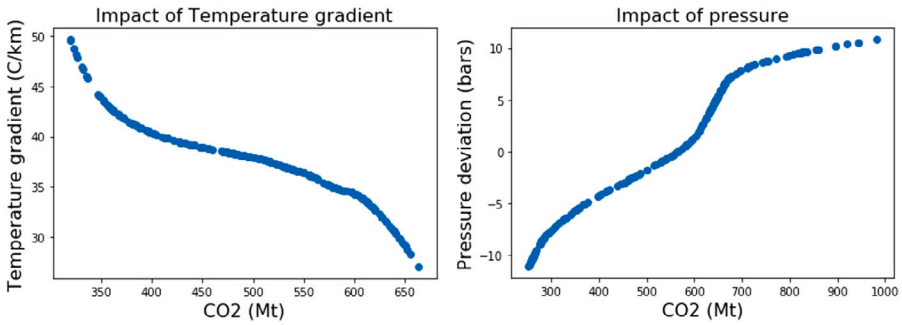

Fig. 4. Impact of pressure and temperature gradient in CO_2 storage capacity.

Table 1
Decision problem setting.

Injection period	60 years
Alternative	Continue or stop the injection at times {14,26,32,40,50,55}
Uncertainty/States	Permeability, porosity, temperature, pressure, and caprock elevation (100 realizations)
Value derived from the decision situation	Net present value
Information data	AVO attributes

In addition, we let $t \in (14, 26, 32, 40, 50, 55)$, and denoted the time in years when the decision of whether to entirely stop the CO_2 injection operation has to be made. We assumed that the injection cannot be resumed once it has stopped. This indicates that the number of decision points in this case is 1200 ($alternatives \times time\ point \times realizations$) (see Table 1).

4.2. Modeling the data and the value outcomes

For each simulation and decision alternative, we extracted CO_2 saturations for each cell in a particular area of the reservoir at different times. This area is marked in blue in Fig. 5 and contains the injection well. We were interested in the saturation at the top of the reservoir to generate the AVO data simulation for each cell. Fig. 6 shows the average saturation for the two scenarios at different times. On average, CO_2 plumes behave differently depending on the injection stop time. However, the injection stopping times are not the only factors that differ between the simulations; they also have different porosities, permeabilities, caprock elevation, temperature, and pressure, which affect the behavior of the plume.

Fig. 7 demonstrates the comparison between CO2 saturation at injection well in two different alternatives (1 : stop injection at 14 years, 7 : stop injection at 60 years) for 100 realizations, one can point out that significant uncertainties are involved.

To estimate the elastic properties and simulate the AVO data, we followed what was presented in the previous section; to estimate the elastic properties of the caprock and initial p- and s-wave velocities at the top of the reservoir, we used well-log data from Dupuy et al. (2017). The initial velocities of the top of the reservoir were estimated by selecting the average value of the velocities over a thickness of 60 m into the reservoir. The estimated values correspond to the values presented by Dupuy et al. (2017). We calculated the initial bulk density of the reservoir for different cells with varying porosities using Eq. 12. The initial velocities of the reservoir may also depend on porosity. Following Dupuy et al. (2017) the authors found that the p-wave velocity decreased rapidly when a small percentage of CO_2 replaced the brine and remained relatively constant for CO_2 saturations greater than 50%. In addition, VS increases with SCO_2, and a linear behavior is shown by the S-wave velocities and bulk density. Variations in the S-wave velocity are limited because VS fluid dependence is found only in the density term (shear modulus is independent of fluid properties). The properties of fluids and minerals are also derived from Dupuy et al. (2017) as shown in Table 2.

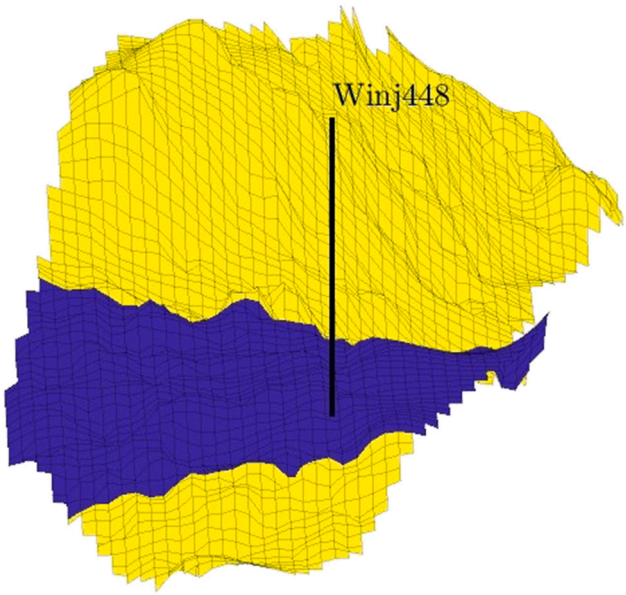

Fig. 5. Reservoir grid, with the area of the seismic survey marked in Blue.

Table 2
Brine, CO_2 properties and rock frame in Utsira sands. The values are derived from (Furre et al., 2017) and (Dupuy et al., 2017).

Properties	Parameter	Value
Utsira sands	K_s (GPa)	39.3
	G_s (GPa)	44.8
	ρ_s (kg/m^3)	2664
Brine	K_w (GPa)	2.31
	ρ_w (kg/m^3)	1030
	η (Pa.s)	0.00069
CO_2	K_{CO_2} (GPa)	0.08
	ρ_{CO_2} (kg/m^3)	700
	η_{CO_2} (Pa.s)	0.000006
Rock frame	m	1
	ϕ	0.37
	k_o (m^2)	2 10–12
	k_D (GPa)	2.56
	G_D (GP)	8.5

Fig. 8 shows the average R_0 attributes for the two different scenarios at different times. Comparing this with Fig. 6, we see that the average

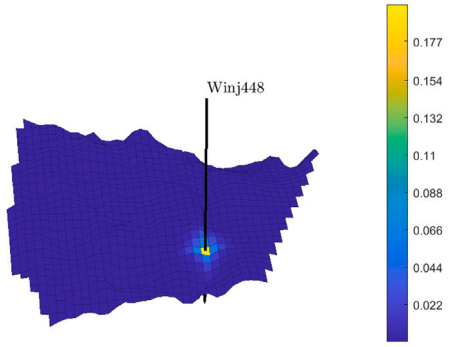

(a) time 14 years.

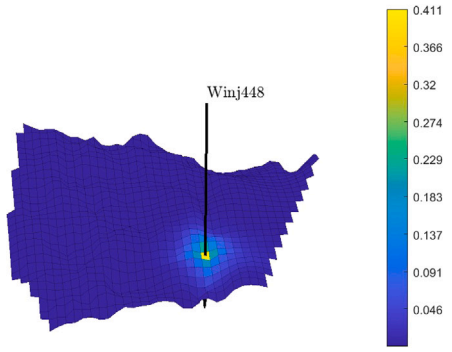

(b) time 50 years.

Fig. 6. Average saturations at times 14 and 50 Years.

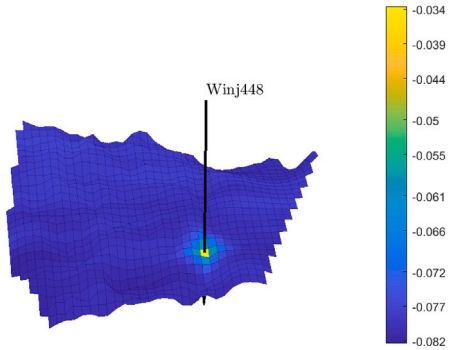

(a) time 14 years.

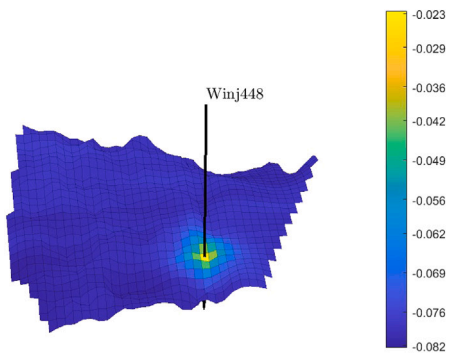

(b) time 50 years.

Fig. 8. Average R_0 attributes at time 14 and 50 years.

of R_0 attributes offers a clear picture of the average saturation. Fig. 9 illustrates the average G attributes for the two different scenarios at different times. Comparing this with Fig. 6, we notice that the average G attributes provide an excellent picture of the average saturation.

To compute the VOI using ADP, the NPV for each decision alternative corresponding to each realization must be evaluated. As our objective is to minimize excess leakage and preserve caprock integrity, the simplest objective function would be measuring the amount of CO_2 injected M_{inj} and penalizing the amount of CO_2 M_{leak} that has left the aquifer through the open boundaries or by leakage through the caprock, which can be associated with project costs and penalty fine if leakage occurs. The NPV function will then conceptually be of the form of the amount of money saved by storing CO_2 minus both the project costs and the penalty fine. For illustration purposes, \$34/t CO_2 would be deployed as the market price in the form of carbon credits to avoid CO2 emissions. Also, \$1.2/t CO_2 would be utilized as a leakage-related fine. The cost of the CO_2 captured is in the range of \$11/t CO_2–\$32/t CO_2 (Puerta-Ortega et al., 2013), this value was fixed at approximately \$25/t CO_2 for our study (Sintef, 2019). Furthermore, \$3.5/t CO_2 was set to cover the costs of construction, operation, and maintenance (Bock et al., 2003). The cost estimate for storage in the onshore USA saline formation is \$2.8/t CO_2 (IPCC, 2005), and the monitoring cost is in the range of \$0.2/t CO_2. The net cost would be then \$25/t CO_2 + \$3.5/t CO_2 + \$2.8/t CO_2 + \$0.2/t CO_2 = \$31.5/t CO_2; hence, the NPV can be expressed as the following:

$$NPV = Revenue - Cost - Penalty$$

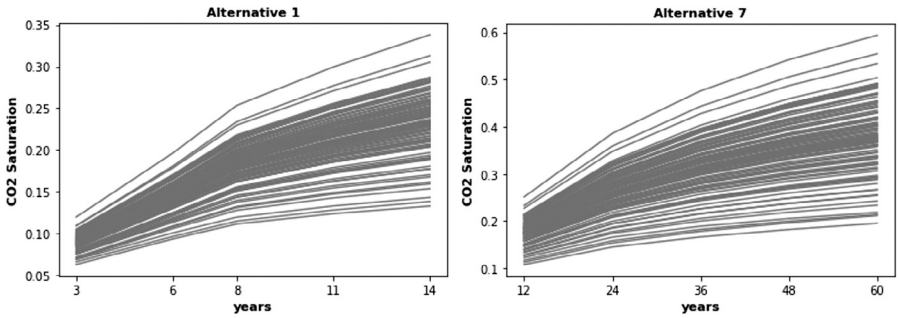

Fig. 7. CO_2 saturation profiles for all realizations: Alternatives 1 and 7.

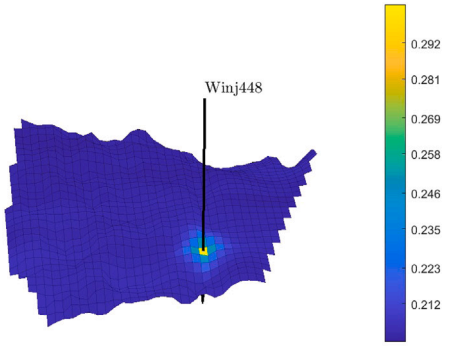

(a) time 14 years.

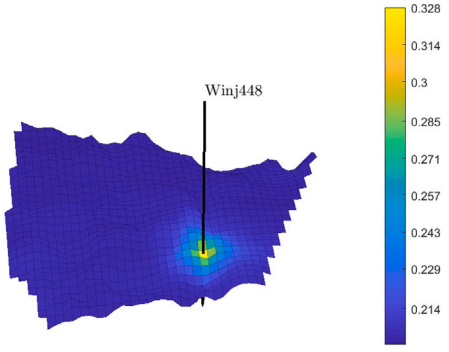

(b) time 50 years.

Fig. 9. Average G attributes at time 14 and 50 years.

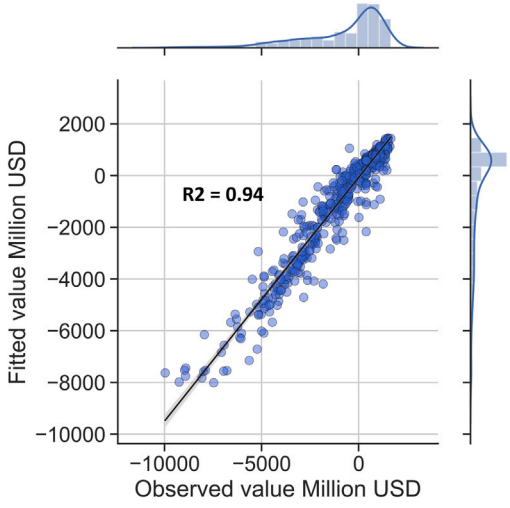

Fig. 10. Plot of fitted values versus observed value using the $R_0 - G$ data.

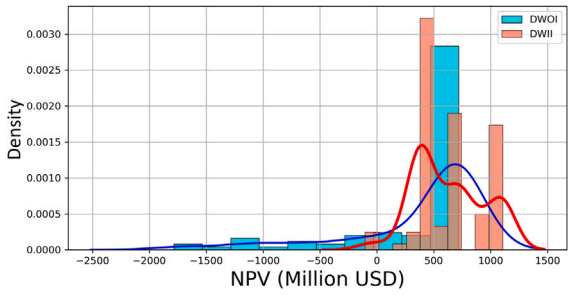

Fig. 11. Graph of PDFs against NPVs with respect to DWOI and DWII.

where,

$$Revenue = \$34/tCO_2 \times (M_{inj} - M_{leak})$$
$$Cost = \$31.5/tCO_2 \times M_{inj}$$
$$Penalty = \$1.2/tCO_2 \times M_{leak}$$

4.3. Value regression using machine learning

To compute the VOI of time-lapse seismic data, we needed to regress the NPVs on the measured AVO attributes for each decision alternative and boundary conditions. We used an automated machine learning (Auto ML) technique called the tree-based pipeline optimization tool (TPOT). The TPOT was first proposed by Olson and Moore (2019). In short, the TPOT optimizes various machine learning pipeline techniques using stochastic search algorithms such as genetic programming. To prevent and reduce overfitting in the machine learning training process, we used 5-fold cross-validation. Cross-validation was run separately for each strategy. Fig. 10 shows a plot of the fitted values using machine learning versus the observed values for the entire sample. A high correlation was observed between the fitted and observed values, with a correlation coefficient of approximately 0.94.

The DWOI is to finish the CO_2 injection by the end of 26 years, and the EVWOI is found to be \$385.63 million. Moreover, the EVWPI is estimated to be \$891.48 million. This pegs the VOPI at \$505.85 million. The highest EVWII corresponding to machine learning was obtained through the Auto ML and provided an EVWII of \$628.46 million, with a related VOI of \$242.85 million. This result indicates that it is uneconomical to proceed with any information-gathering activity if it costs more than \$242.85 million. This result also illustrates that including the effect of future information and decisions could improve the EV by 62.97%, which is the percentage of the fraction of VOI to EVWOI.

The probability density function (PDF) of NPVs associated with DWOI and DWII are plotted in Fig. 11. From this figure, we notice that the NPV resulting from the ML approach (DWII) is higher than that of the DWOI. In this aspect, integrating the effects of future information and decisions in decision-making would increase the ENPV. Some realizations end up with a smaller NPV with DWII than the NPV with DWOI, which may be due to a suboptimal decision, as the machine learning algorithm is the approximate method, which, for some of the path decisions, makes suboptimal choices.

The normalized frequency distribution (NFD) of the CO_2 injection is illustrated in Fig. 12. Based on these results, it is more worthwhile to cease CO_2 injection between 14 and 40 years (i.e., there is a 38% and 32% chance that the CO_2 injection mechanism should be stopped at the end of 14 and 26 years, respectively). There is only a 22% less chance that it is optimal to stop the same after 40 years. The specific stop time depends mainly on the measured seismic data and geological realization, including the uncertainty in permeability, porosity, caprock elevation, pressure, and temperature.

4.4. Sensitivity analysis in AVO attributes

The next step is to assume the AVO attributes R_0 and G to be noisy and normally distributed:

$$(R_0, G)^T \approx \mathcal{N}(m, T)$$

where the mean m is calculated using Eqs. 11 and 12. Following Eidsvik et al. (2015), the covariance matrix corresponding to the one set for the

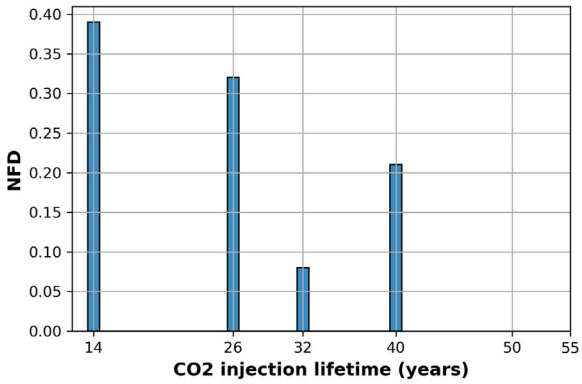

Fig. 12. NFDs of the CO_2 optimal stop injection time corresponding to the decision-making with ML.

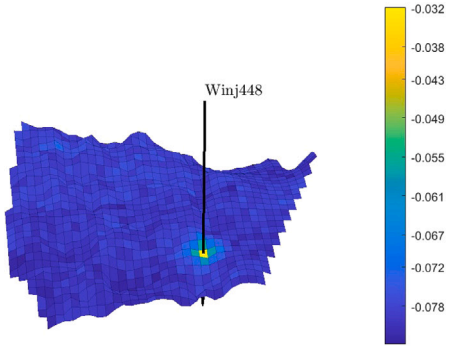

(a) time 14 years.

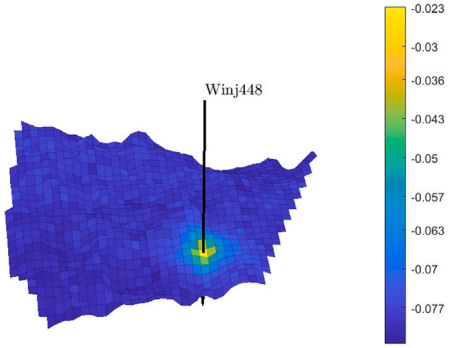

(b) time 50 years.

Fig. 13. Average R_0 attributes at times 14 and 50 years.

likelihood model for AVO data was set to the following:

$$T = c \begin{pmatrix} 0.06^2 & -0.7 \times 0.06 \times 0.17 \\ -0.7 \times 0.06 \times 0.17 & 0.17^2 \end{pmatrix}$$

Where c > 0.

Figs. 13 and 14 demonstrate R_0 and G attributes, respectively, for the two different scenarios. Comparing these with Fig. 6, which contains the same simulations, we observe that the R_0 attributes present an effective picture of the saturation; however, there is significant noise for the R_0 attributes. This is expected as the variance is higher for G than for R_0.

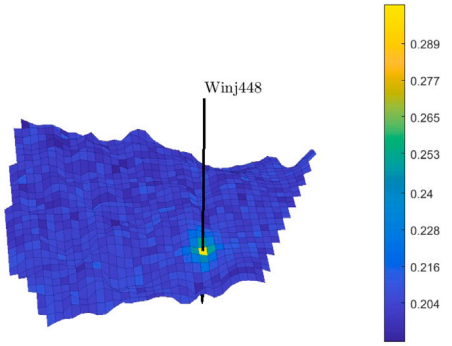

(a) time 14 years.

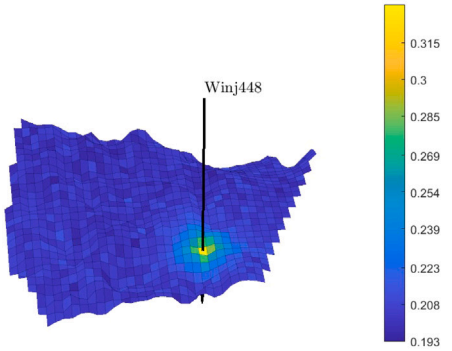

(b) time 50 years.

Fig. 14. Average G attributes at times 14 and 50 years.

By adding uncertainty in AVO attributes, the EVWII is estimated to be $617.11 million. This makes the VOI $231.48 million. This result indicates that it is uneconomical to proceed with any information-gathering activity if it costs more than $231.48 million. This result also illustrates that including the effect of future information and decisions could improve the EV by 60.03%, which is the percentage of the fraction of VOI to EVWOI.

The NFDs of the total lifetime corresponding to the decisions with machine learning are displayed in Fig. 16. This result recommends stopping CO_2 injection at the end of years 14 and 26 (i.e., there is more than a 60% chance that the CO_2 injection mechanism should be stopped after year 26). There is only less than 5% chance that it will be optimal to stop the injection after 32 and 40 years. The specific stop time depends mainly on the perturbed measured seismic data and uncertainty of geological realization.

Fig. 15 shows a comparison of the PDFs corresponding to the different methods. The NPV resulting from the ML approach (DWII) is higher than that of the DWOI, as ML allows learning over time. Moreover, some realizations resulted in a smaller NPV with ML than with the DWOI. This may be due to suboptimal decisions.

4.4.1. Sensitivity analysis in carbon price

In both previous studies, we did not include uncertainties in the carbon price, even though it significantly impacted the decision. Therefore, in this work, the carbon price was treated as an uncertain parameter and considered in the regression analysis to determine the optimal stopping time in CO_2 injection monitoring.

The carbon price is modeled as Markovian processes and variants over time. Hence, it is assumed to follow a stochastic process. There are two commonly used stochastic models to describe uncertainties in

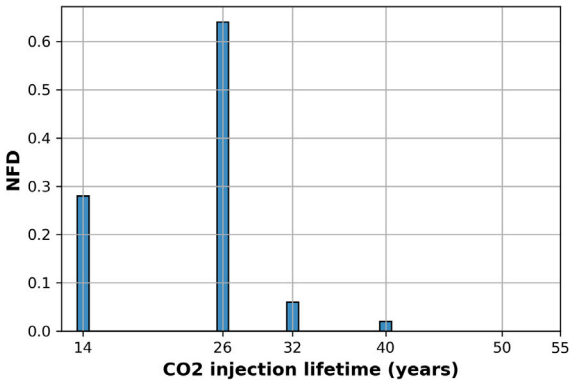

Fig. 15. NFDs of the CO_2 optimal stop injection time corresponding to the decision-making with ML.

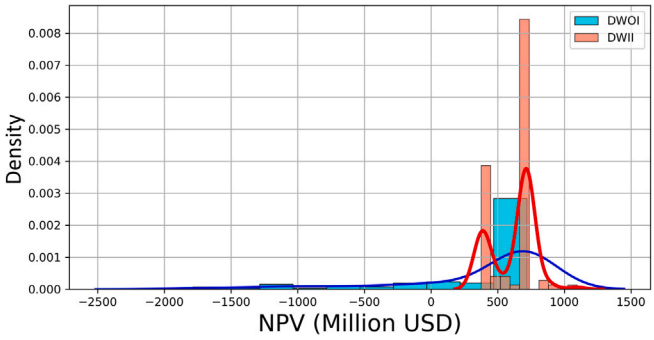

Fig. 16. Graph of PDFs against NPVs with respect to DWOI and DWII.

economic variables: the geometric Brownian motion (also known as the random-walk model) and the Ornstein–Uhlenbeck (OU) stochastic process (also known as the mean-reverting model; refer to Uhlenbeck and Ornstein (1930) for more details).

A process "S" can be stochastically modeled using the Ornstein–Uhlenbeck process as shown below:

$$dS_t = \theta\,(\mu - S_t)dt + \sigma dW_t \tag{15}$$

where θ is the speed of mean reversion, μ is the long-term mean which the process reverts, σ is the measure of process volatility, and W_t stands for a Brownian motion, where $dW_t \sim N(0, \sqrt{d_t})$. This stochastic equation must be discretized to be implemented in the simulation. Gillespie (1996) opined that the simulation of the process would work well only when the discretized time Δ_t is sufficiently small. Thus, the discretized equation is as follows:

$$S_t = (S_{t-1} \times e^{-\theta\Delta t}) + \mu(1 - e^{-\theta\Delta t}) + \left[\sigma \times \sqrt{\frac{1 - e^{-2\theta\Delta t}}{2\theta}} \times dW_t\right] \tag{16}$$

However, if any commodity price, including carbon prices per unit, or any other cost is modeled using the above discrete-time expression, negative values might be generated. This is not realistic, because negative commodity prices never exist. To avoid this problem, we used the lognormal distribution of commodity prices. Thus, in this context, the logarithm of the modeled parameter, namely $\pi_t = ln[St]$, is assumed to follow the mean-reverting process. This process can be mathematically described as follows:

$$d\pi_t = \kappa[\bar{\pi} - \pi_t]d_t + \sigma\pi dz_t \tag{17}$$

where κ is the speed of mean reversion, $\bar{\pi}$ is the long-term mean that the logarithm of the variable reverts, $\sigma\pi$ stands for the volatility of process, and dz_t describes the increments of standard Brownian motion. Subsequently, to numerically solve for π_t, the stochastic equation is

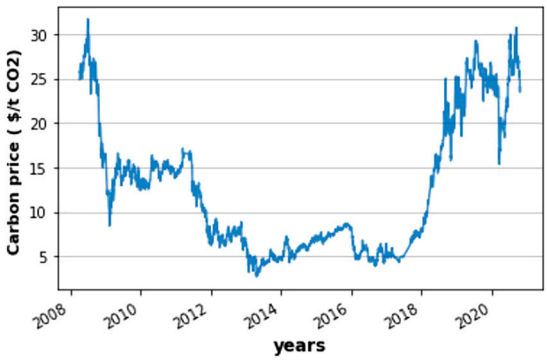

Fig. 17. Historical of carbon prices from 1985 to 2021.

discretized as shown below (by assuming $dz_t \sim (0, \sqrt{d_t})$, where d_t = 1 year).

$$\pi_t = (\pi_{t-1} \times e^{-\kappa\Delta t}) + \bar{\pi}(1 - e^{-\kappa\Delta t}) + \left(\sigma_\pi \times \sqrt{\frac{1 - e^{-2\kappa\Delta t}}{2\theta}} \times N(0,1)\right) \tag{18}$$

After calculating π_t, the value of S_t cannot directly be obtained using the equation of $S_t = e^{\pi t}$. This is due to the fact that half of the variance is added to the mean of the lognormal distribution, namely $0.5 \times var(\pi_t)$, for the exponential of a normal distribution. Therefore, half of the variance is deducted using the following equation:

$$Var(\pi_t) = [1 - e^{-\kappa\Delta t}] \times \frac{\sigma_\pi{}^2}{2\kappa} \tag{19}$$

To use this model, a decision must be made to determine its parameters. This process is known as calibration, and since the logarithm of the variables is assumed to follow the mean-reverting process, the least-squares regression, which was suggested by Smith (2010), was conducted on the datasets of $\pi_t = ln[S_t]$. To calibrate the OU parameters for the modeling of the carbon credit price, a set of carbon credit price data is required. For illustration, the annual carbon credit price data, namely prices from 2008 to 2020 (considering only historical data), which is available on the European Union Emissions Trading System carbon market price European Union Emissions Trading System carbon market price (2021), were used as displayed in Fig. 17.

To start the procedure of calibration, we used the following equations:

$$x_t = \pi_t - \Delta_t = ln[Pt - \Delta_t] \tag{20}$$

$$y_t = \pi_t = ln[Pt] \tag{21}$$

$$y_t = ax_t + b + \delta \tag{22}$$

The OU parameters are estimated using the values of a and b:

$$\bar{\pi} = \frac{b}{1-a},\ \kappa = \frac{-ln\ a}{\Delta t},\ \sigma_\pi = \sigma_\delta \sqrt{\frac{-2ln\ a}{\Delta t(1-a^2)}} \tag{23}$$

where δ is the approximation error introduced in the least-squares regression, σ_δ is the standard deviation of the approximation errors, and Δt is the difference in two time-steps. Refer to Smith (2010) for more details regarding the derivation of the equations.

Using the parameters in Table 3, the carbon price corresponding to the respective costs is modeled forward in time. Fig. 18 presents the probabilistic model of the oil price.

By adding uncertainty in the carbon price, the DWOI provides 14 years CO_2 injection time, and the EVWOI is found to be $432.50 million. Moreover, the highest EVWII corresponding to machine learning was $870.23 million, which also illustrates that including the effect of future information and decisions improves the net present value. The

Table 3
Values of parameters used in the mean-reverting model.

Parameter	Carbon price
Initial value	34
Equilibrium value	34
Volatility σ_δ	0.4811
Mean reversion speed, κ	0.2647
d_t, year	1

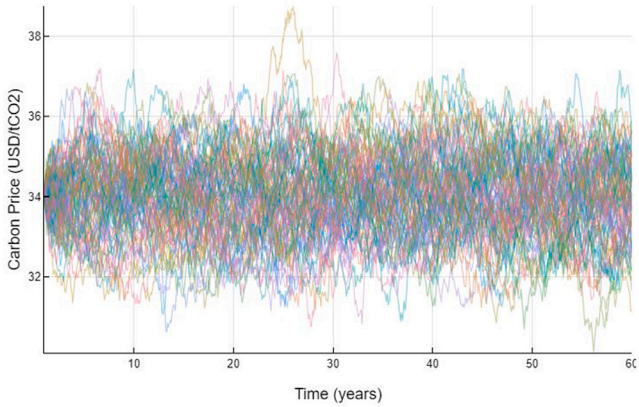

Fig. 18. Carbon prices modeled using the mean-reverting process.

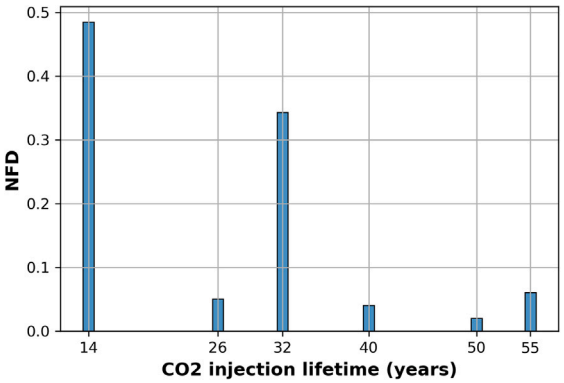

Fig. 19. NFDs of the CO_2 optimal stop injection time corresponding to the decision-making with ML.

NFDs of the total lifetime corresponding to the decision with machine learning are shown in Fig. 20. This result recommends stopping CO_2 injection mostly at the end of years 14 or 32 (i.e., there is a more than 32% chance that the CO_2 injection mechanism should be stopped after years 14 and 32). There is only a less than 10% chance that it is optimal to stop the injection after 26, 40, 50, and 55 years. The specific switch time depends mainly on the uncertainty of geological realization and perturbed modeled AVO attributes, including uncertainty in carbon prices.

Fig. 19 shows a comparison of the PDFs of NPVs associated with DWOI and DWOII. The NPV resulting from the ML approach (DWII) is higher than that of the DWOI, as ML allows learning over time. Furthermore, some realizations resulted in a smaller NPV with ML than with the DWOI. This may be due to suboptimal decisions.

5. Discussion and concluding remarks

We presented a VOI framework that can be used to compute the VOI in a reservoir development plan. Specifically, we applied the framework to evaluate the VOI of time-lapse seismic data in the context

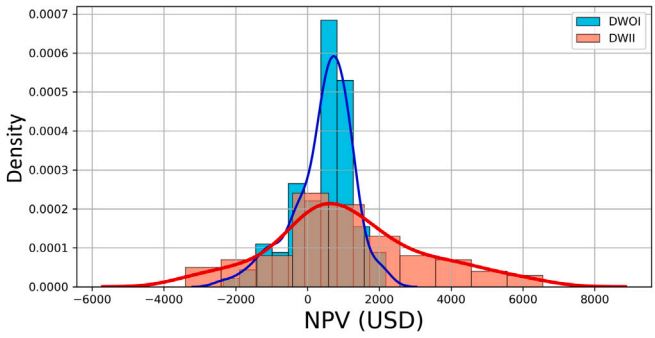

Fig. 20. Graph of PDFs against NPVs with respect to DWOI and DWII.

of CO_2 storage and the detection of potential CO_2 leakage. A case has been developed where, based on information from seismic surveys and carbon credit prices, a decision-maker must decide on the best time to continue or stop the CO_2 injection. The reliability of a seismic survey and carbon prices are likely to increase with time and the amount of CO_2 injected into the reservoir. In this context, the decision of when to perform the survey becomes a trade-off between test reliability and the amount of CO_2 at risk of leakage. For this study, we used the Utsira field CO_2 storage atlas, which is located in the North Sea, and considered a storage location for the full-scale Norwegian CCS project. We used an approximate dynamic approach to estimate the VOI for seismic surveys. Nevertheless, when a seismic survey is most important, the VOI estimates do not provide an accurate response. Notwithstanding, we may tentatively claim that in the injection phase, a seismic survey should not be performed too early or too late. In addition, the value of learning induced by machine learning may be small and insignificant, as there is always an approximation error when applying the machine learning regression function. In addition, the closeness of a regression function to estimate the actual expected values and the accuracy of this method mainly depend on the prior sample of Monte Carlo, alternatives, and information, and, in some cases, the model choice may not be material.

In conclusion, the VOI framework can generally be applied to any type of spatial data and in the context of decisions other than reservoir development. The framework can be evaluated as an interplay between three key factors: the decision-making situation consisting of alternatives and prospect values, the uncertain variables of interest that affect the prospect values, and the data that informs about these variables of interest. Moreover, the approximate dynamic methodology can be applied to estimate the conditional expectation of prospect values given the data outcomes, and thereby to evaluate the VOI. This computational efficiency of ADP allows VOI computation in complex decision situations where the rigorous Monte Carlo methodology is intractable. However, the VOI is still quite uncertain, and to consistently estimate the VOI in complex sequential decision cases, it might be beneficial to increase the number of realizations or reduce the number of alternatives in innovative ways. Therefore, a new procedure and methodology based on clustering techniques, in combination with proxy models, must be developed to reduce computational costs and efficiently solve real-world sequential decision-making problems.

CRediT authorship contribution statement

Amine Tadjer: Wrote the paper, Contributed to tuning the model, Analyzing the results. **Aojie Hong:** Supervised the work, Providing continuous feedback. **Reidar B. Bratvold:** Supervised the work, Providing continuous feedback.

Declaration of competing interest

The authors declare that they have no known competing financial interests or personal relationships that could have appeared to influence the work reported in this paper.

Acknowledgments

The author acknowledges financial support from the Research Council of Norway through the Petromaks-2 project DIGIRES (RCN no. 280473) and the industrial partners AkerBP, Wintershall DEA, ENI, Petrobras, Equinor, Lundin, and Neptune Energy. All authors have read and agreed to the published version of the manuscript.

References

Allen, R., Nilsen, H., Lie, K., O., M., Andersen, O., 2018. Using simplified methods to explore the impact of parameter uncertainty on CO_2 storage estimates with application to the Norwegian Continental Shelf. Int. J. Greenhouse Gas Control 75, 198–213.

Andersen, O., Nilsen, H., Lie, K.A., 2014. Reexamining CO_2 storage capacity and utilization of the utsira formation. 2014, 1–18.

Anyosa, S., Bunting, S., Eidsvik, J., Romdhane, A., Bergmo, P., 2021. Assessing the value of seismic monitoring of CO_2 storage using simulations and statistical analysis. Int. J. Greenhouse Gas Control 105, 103219. http://dx.doi.org/10.1016/j.ijggc.2020.103219, URL: https://www.sciencedirect.com/science/article/pii/S1750583620306447.

Arts, R., Eiken, O., Chadwick, A., Zweigel, P., Van der Meer, L., Zinszner, B., 2004. Monitoring of CO_2 injected at sleipner using time-lapse seismic data. Energy 29, 1383–1392. http://dx.doi.org/10.2118/65148-MS.

Avseth, P., Mukerji, T., Mavko, G., 2005. Quantitative Seismic Interpretation: Applying Rock Physics Tools To Reduce Interpretation Risk. Cambridge University Press, http://dx.doi.org/10.1017/CBO9780511600074.

Aylor Jr., W., 1999. Measuring the impact of 3D seismic on business performance. J. Petrol. Techno 51 (6), 52–56. http://dx.doi.org/10.2118/56851-JPT.

Bickel, J.E., Gibson, R.L., McVay, D.A., Pickering, S., R, J., 2008. Quantifying the reliability and value of 3D land seismic. SPE Res. Eval. Eng. 11, 832–841. http://dx.doi.org/10.2118/102340-PA.

Bock, B., Rhudy, R., Herzog, H., Klett, M., Davison, J., Ugarte, D.G.D.L.T., Simbeck, D., 2003. Economic evaluation of CO_2 storage and sink enhancement options. http://dx.doi.org/10.2172/826435, URL: https://www.osti.gov/biblio/826435.

Bratvold, R., Bickel, J., Lohne, H., 2009. Value of information in the oil and gas industry : Past, Present, and Future. SPE Reserv. Eval. Eng. 2 (4), 630–638. http://dx.doi.org/10.2118/110378-PA.

Dupuy, B., Ghaderi, A., Querendez, E., Mezyk, M., 2017. Constrained AVO for CO_2 storage monitoring at sleipner. Energy Procedia 114, 3927–3936. http://dx.doi.org/10.1016/j.egypro.2017.03.1524.

Dutta, G., Mukerji, T., Eidsvik, J., 2019. Value of information analysis for subsurface energy resources applications. Appl. Energy 252, 113436. http://dx.doi.org/10.1016/j.apenergy.2019.113436.

Eidsvik, J., Dutta, G., Mukerji, T., Bhattacharjya, D., 2017. Simulation–regression approximations for value of information analysis of geophysical data. Math. Geosci. 49 (4), 467–491. http://dx.doi.org/10.1007/s11004-017-9679-9.

Eidsvik, J., Mukerji, T., Bhattacharjya, D., 2015. Value of Information in the Earth Sciences. Cambridge Univeristy Press, Cambridge.

European Union Emissions Trading System carbon market price, 2021. Daily EU ETS carbon market price (Euros). URL: https://ember-climate.org/data/carbon-price-viewer/.

Furre, A.-K., Eiken, O., Alnes, H., Vevatne, J.N., Kiær, A.F., 2017. 20 years of monitoring CO_2-injection at sleipner. Energy Procedia 114, 3916–3926. http://dx.doi.org/10.1016/j.egypro.2017.03.1523.

Gassmann, F., 1951. Über die elastizität poröser medien: Vierteljahrsschrift der Naturforschenden Gesellschaft in Zurich. 96, pp. 1–23.

Gillespie, D., 1996. Exact numerical simulation of the Ornstein-Uhlenbeck process and its integral. Geosci. Data J. 54, 2084–2091. http://dx.doi.org/10.1103/PhysRevE.54.2084.

Han, D.-H., Batzle, M., 2004. Gassmann's equation and fluid-saturation effects on seismic velocities. GEOPHYSICS 69 (2), 398–405. http://dx.doi.org/10.1190/1.1707059, arXiv:https://doi.org/10.1190/1.1707059.

Harp, D.R., Stauffer, P.H., O'Malley, D., Jiao, Z., Egenolf, E.P., Miller, T.A., Martinez, D., Hunter, K.A., Middleton, R., Bielicki, J., 2017. Development of robust pressure management strategies for geologic CO_2 sequestration. Int. J. Greenhouse Gas Control 64, 43–59.

Hong, A., Bratvold, R., Lake, L., 2018a. Fast analysis of optimal IOR switch time using a two-factor production model and least- squares Monte Carlo algorithm. SPE Reserv. Eval. Eng. http://dx.doi.org/10.2118/191327-PA.

Hong, A., Bratvold, R., Thomas, P., Hanea, R., 2018b. Value-of-information for model parameter updating through history matching. J. Pet. Sci. Eng. 165, 253–268. http://dx.doi.org/10.1016/j.petrol.2018.02.004, URL: https://www.sciencedirect.com/science/article/pii/S0920410518300998.

Howard, R., 1966. Information value theory. IEEE Trans. Syst. Sci. Cybern. 2 (1), 22–26. http://dx.doi.org/10.1109/TSSC.1966.300074.

Jafarizadeh, B., Bratvold, R., 2009. Taking real options into real world: Asset valuation through option simulation. In: SPE Annual Technical Conference and Exhibition. New Orleans, Louisiana, http://dx.doi.org/10.2118/124488-MS.

Jin, L., Hawthorne, S., Sorensen, J., Pekot, L., Kurz, B., Smith, S., Heebink, L., Hergegen, V., Bosshart, N., Torres, J., Dalkhaa, C., Peterson, K., Gorecki, C., Steadman, E., Harju, J., 2017. Advancing CO_2 enhanced oil recovery and storage in unconventional oil play—Experimental studies on bakken shales. Appl. Energy 208, 171–183.

Lie, K.-A., 2019. An Introduction To Reservoir Simulation using MATLAB/GNU Octave: User Guide for the MATLAB Reservoir Simulation Toolbox (MRST). Cambridge University Press, http://dx.doi.org/10.1017/9781108591416.

Longstaff, F., Schwartz, E., 2001. Valuing American options by simulation: a simple least-squares approach. Rev. Financ. Stud. 14 (1), 113–147. http://dx.doi.org/10.1093/rfs/14.1.113.

Newendorp, P., 1975. Decision analysis for petroleum exploration. URL: https://www.osti.gov/biblio/7318461.

Nguyen, P., Nam, M., 2011. Review on methods for constructing rock physics model of saturated reservoir rock for time-lapse seismic. Geosyst. Eng. 14 (2), 95–107. http://dx.doi.org/10.1080/12269328.2011.10541336.

Nilsen, H., Lie, K.A., Andersen, O., 2015a. Analysis of CO_2 trapping capacities and long-term migration for geological formations in the Norwegian North Sea using MRST-co2lab. Comput. Geosci. 79, 15–26.

Olson, R., Moore, J., 2019. A tree-based pipeline optimization tool for automating machine learning. In: Hutter F., V.J. (Ed.), Automated Machine Learning. In: The Springer Series on Challenges in Machine Learning, Springer.

Puerta-Ortega, C., Bickel, J.E., Hovorka, S., 2013. Assessing the value of permeability data in a carbon capture and storage project. Int. J. Greenhouse Gas Control 17, 523–533. http://dx.doi.org/10.1016/j.ijggc.2013.06.003, URL: https://www.sciencedirect.com/science/article/pii/S175058361300251X.

Raiffa, H., Schlaifer, R., 1961. Applied Statistical Decision Theorys. Harvard University, Wiley.

Riis, T., 1999. Quantifying the value of information. Pet. Eng. Int. 72 (6), URL: https://www.osti.gov/biblio/354456.

Sato, K., 2011. Value of information analysis for adequate monitoring of carbon dioxide storage in geological reservoirs under uncertainty. Int. J. Greenhouse 5 (5), 1294–1302. http://dx.doi.org/10.1016/j.ijggc.2011.07.010.

Singh, V., Cavanagh, A., Hansen, H., Nazarian, B., Iding, M., Ringrose, P., 2010. Reservoir modeling of CO_2 plume behavior calibrated against monitoring data from sleipner, Norway. In: SPE Annual Technical Conference and Exhibition. Florence, Italy, Society of Petroleum Engineers.

Smith, W., 2010. On the simulation and estimation of the mean-reverting Ornstein-Uhlenbeck process. URL: https://commoditymodels.files.wordpress.com/2010/02/estimating-the-parameters-of-a-mean-reverting-ornsteinuhlenbeck-process1.pdf.

Uhlenbeck, G., Ornstein, L., 1930. On the theory of the Brownian motion. Phys Rev 36, 823–841. http://dx.doi.org/10.1103/PhysRev.36.823.

Waggoner, J., 2000. Lessons learned from 4D projects. SPE Reserv. Eval. Eng. 3 (4), 310–318.

Wood, A., 1941. A Textbook of Sound. G. Bell and Sons LTD, London.